Experimental and Theoretical Investigation of the Mechanism of Radiation-Induced Radical Formation in Hydrogen-Bonded Cocrystals of 1-Methylcytosine and 5-Fluorouracil

David M. Close,*,† Leif A. Eriksson,‡ Eli O. Hole,§ Einar Sagstuen,§ and William H. Nelson¶

Physics Department, East Tennessee State University, P.O. Box 70652, Johnson City, Tennessee 37614, Department of Quantum Chemistry, Box 518, Uppsala University, S-751 20 Uppsala, Sweden, Department of Physics, University of Oslo, P.O. Box 1048, Blindern, N-0316 Oslo, Norway, and Department of Physics and Astronomy, Georgia State University, Atlanta, Georgia 30303

Received: May 17, 2000; In Final Form: July 20, 2000

The process of stabilizing radiation damage in the base pair of 1-methylcytosine (1-MeC):5-fluorouracil (5-FU) has been investigated. The formation of free radicals in purines and pyrimidines is influenced by the matrix in which they are irradiated. Of particular interest are the systems in which two different nucleic acid bases are complexed, providing situations that approximate the close proximity of bases in nucleic acid polymers. Detailed EPR/electron−nuclear double resonance experiments show that only the N3 protonated cytosine anion and the N1 deprotonated uracil cation are observed in single crystals of 1-MeC:5-FU, X-irradiated, and observed at 10 K. Upon warming one observes a radical formed by net hydrogen addition to C6 on uracil, and an allylic radical on the C4−C5−C6 region of the uracil. No cytosine C5 or C6 H-addition radicals are observed. The implications that free radical damage is transferred from the cytosine moiety to the uracil moiety in 1-MeC:5-FU is discussed. Single point calculations were performed on the optimized geometries at the B3LYP/6-311G(2df,p) level to obtain accurate energies and spin populations. To obtain electron affinities of the neutral parent molecules, the larger 6-311+G(2df,p) basis set was used. Results show that the cytosine base will be the preferred site of electron addition, and the uracil base will be the site of electron loss. Additional studies were performed to investigate the influence of the hydrogen-bonded crystal matrix on the stabilities of the initial radical ions. On the basis of these studies, a proton shuttle mechanism is proposed that provides an efficient transfer of charge away from the initial sites of electron addition or electron loss, leaving behind neutral radical sites that are less susceptible to recombination.

Introduction

The formation of free radicals in purines and pyrimidines is influenced by the matrix in which they are irradiated. Of particular interest are the systems in which two different nucleic acid bases are complexed, providing situations that approximate the close proximity of bases in nucleic acid polymers. Base pair complexes can reveal the individual roles of hydrogen bonding and base stacking. As such, these are important model systems which extend and supplement information already available from studies of single bases, nucleosides, and nucleotides.

In two previous studies, the radicals detected at 77 and 300 K in X-irradiated single crystals of a molecular complex of 1-methylcytosine (1-MeC) and 5-fluorouracil (5-FU) were identified.[1,2] At 77 K the dominant radical (**R1**) is an oxidation product formed by net hydrogen abstraction from the N1 position of 5-FU.[1] Radical **R1** decays when the crystal is warmed to 220 K. If the crystal is further warmed to room temperature, the EPR spectrum is dominated by radical **R2**, formed by net H-addition to C6 of 5-FU. This radical is actually already present at 77 K, but is most easily studied after warming.

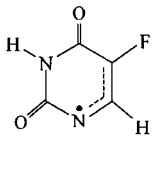

R1

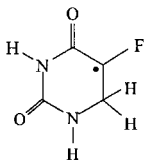

R2

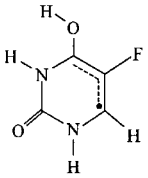

R3

A third radical (**R3**), seen most clearly in crystals irradiated at room temperature, was postulated to be a reduction product formed on 5-FU.[2] New information about radical **R3** is presented in this study. Therefore, to date, all three radicals detected in this molecular complex involve only the uracil moiety.

For the present analysis it will be helpful to compare the results observed in the cocrystalline complex with the results previously observed in the individual bases. Much is already known about the radiation chemistry of 1-MeC. Wyard and Elliott characterized the C5−H addition radical (**R4**) in 1-MeC at room temperature.[3] Rustgi and Box have characterized both radical **R4** and the C6 H-addition radical (**R5**) with electron−nuclear double resonance (ENDOR).[4] Also, a radical anion (or possibly the protonated radical anion) has been detected at 6 K in 1-MeC.[5] A summary of the characteristics of cytosine reduction products has recently been presented.[6] Neumüller and Hüttermann have detected two radical species at 300 K in irradiated 5-FU: a C6−H adduct (**R2**) and a C4−OH radical

* To whom correspondence should be addressed. E-mail: CLOSED@ETSU.EDU.
† East Tennessee State University.
‡ Uppsala University.
§ University of Oslo.
¶ Georgia State University.

10.1021/jp0018246 CCC: $19.00
Published on Web 09/13/2000

(**R3**).[7] At 77 K the EPR spectrum of 5-FU was tentatively assigned to the 5-FU anion.

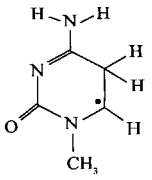

R4

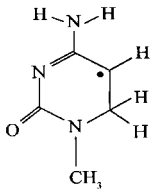

R5

In this study, a cytosine reduction product is found to be present along with the previously observed uracil oxidation product radical **R1** at 10 K. From previous work involving cytosine derivatives, one could expect to observe cytosine C5═C6 H-adducts (either radical **R4** or **R5**).[5] However, no cytosine H-addition radicals were observed in the 1-MeC:5-FU complex. The implication that free radical damage is somehow transferred from the cytosine moiety to the uracil moiety will be discussed herein.

Bernhard et al. recently considered the stability of radicals in various crystalline environments.[8] For example, 1-MeC is known to have a very low radical yield, so it is argued that a large percentage of the initial radicals formed by the ionizing radiation must recombine. Looking at the hydrogen-bonding network of 1-MeC, one sees that the network does not favor long-range proton displacements. Consequently, there are no energetically favorable paths that would promote the separation of unpaired spin and charge, leaving the initial sites prone to recombination. It will be shown, on the other hand, that in 1-MeC:5-FU there are efficient pathways for returning ionization sites to their original charge states, thereby effectively inhibiting recombination.

Materials and Methods

Single crystals of 1-MeC:5-FU were prepared and mounted as described previously.[2] A complete X-ray crystallographic study of 1-MeC:5-FU was reported by Kim and Rich.[9] Our results are expressed in the orthogonal coordinate system based on the orthorhombic unit cell axes $\langle a \rangle$, $\langle b \rangle$, $\langle c \rangle$. Calculations of specific directions in the undamaged molecule were performed with a modified version of the crystallographic program ORFEE.[10]

The crystals were X-irradiated with 50-kV X-rays for 1−2 h at 10 K. Under these conditions the crystals received a dose of approximately 50 kGy. Methods of EPR and ENDOR data collection have been described previously,[11,12] as have methods of data reduction and error analysis.[11] Dose-response curves were determined from two different crystal samples. The average free radical yield at 4 K for 1-MeC:5-FU was 0.038 ± 0.009 μmol/J.[13]

As a complementary tool to assist in the assignments of the observed radicals, the geometries, energetics and hyperfine properties of all possible radicals of 1-MeC and 5-FU, formed via net hydrogen atom abstraction (deprotonated cations) or addition (protonated anions) were investigated theoretically. In addition, the parent molecules and their various tautomers, and the parent radical anions and cations were included in the studied set. All systems were optimized using the hybrid Hartree−Fock−density functional theory functional B3LYP,[14−16] in conjunction with the 6-31G(d,p) basis set of Krishnan et al.[17] Frequency calculations were performed at the same level of theory to ensure that the systems represent true minima on the potential energy surfaces.

Single point calculations were performed on the optimized geometries, at the B3LYP/6-311G(2df,p) level, to obtain accurate energies and spin properties. The single point energetics were corrected for zero-point vibrational effects, as determined at the level of optimization. In the investigation of electron affinities of the neutral parent molecules, the larger 6-311+G(2df,p) basis set was used, because diffuse functions can have a great effect on this property.[18,19] To investigate the effect of the surrounding matrix on the radical systems, the crystal environment was modeled using the polarized continuum model (PCM) of Tomasi et al.[20−24] All calculations were performed using the Gaussian 98 program package.[25]

The positions of the equilibria for the different reactions are governed by the standard free energies of reaction,

$$\Delta\Delta G = \Delta E + \Delta ZPE + \Delta(H_T - H_O) - T\Delta S$$

where ΔE is the difference in electronic energies, ΔZPE is the difference in zero-point energy, $\Delta(H_T - H_O)$ is the difference in heat content, and ΔS is the entropy difference. T is the temperature, which in the present case is 10 K. The contributions from the enthalpy and entropy terms, however, are less than one tenth of a kilocalorie at this temperature, and are neglected in this study.

The combination of methods and basis sets used in this work have previously been used very successfully for determination of geometric structures, relative energies of different conformers, and radical hyperfine coupling constants.[26−29] Overviews of the equations used for evaluating the different components of the diagonalized hyperfine interaction tensor within the density functional theory (DFT) framework, and their performance, have been presented by Malkin et al.[30] and by Barone.[31]

Results and Analysis

Cytosine Anion. The second derivative K-band EPR spectra of a single crystal of 1-MeC:5-FU, X-irradiated and observed at 10 K is shown in Figure 1a. One clearly sees resonance patterns from two radical species. The outer lines from radical **R1** exhibit a large α-fluorine coupling and an additional nitrogen coupling as described previously.[1]

In the center of the spectra shown in Figure 1a is a broad doublet (radical **R6**) with a hyperfine splitting of approximately 1.5 mT. This doublet exhibits noticeable anisotropy as the crystal is rotated in the external magnetic field. Unfortunately there is severe overlap with the lines from radical **R1** at orientations where the α-fluorine coupling is small. It was therefore necessary to perform a detailed ENDOR experiment on the EPR lines from this doublet.

ENDOR lines from radical **R6** were detected in the range from 35 to 65 MHz (Figure 1b) by microwave power saturating the central region of the K-band EPR spectrum shown in Figure 1a. The angular variation of the ENDOR lines in three mutually perpendicular planes was measured. The angular variation of the largest coupling is typical of an α-hydrogen hyperfine coupling as seen by the principal values of the hyperfine coupling tensor given in Table 1 (**6a**). From the known crystal structure of the complex[9] one can calculate the perpendicular to the base rings (the expected direction of the π-orbital) and a few key C−H bond directions. The hyperfine coupling data in Table 1 agree almost exactly with the directions calculated for the C6−H_α coupling on 1-MeC.

The Field Swept ENDOR (FSE) spectrum of coupling **6a** shows a 1.7-mT doublet for the external magnetic field H_o // $\langle c \rangle$. An identical FSE spectrum was seen for an ENDOR line

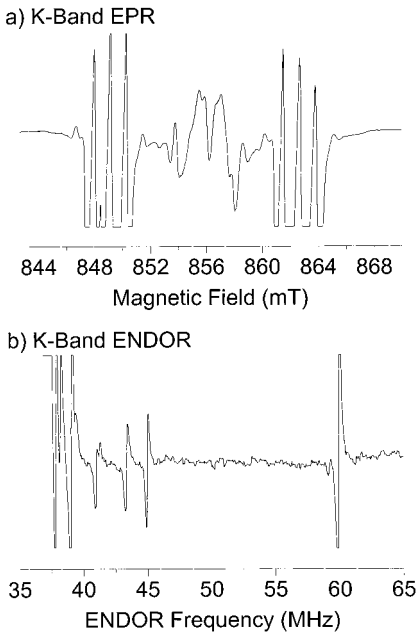

Figure 1. (a) K-band EPR spectrum of a single crystal of 1-MeC:5-FU X-irradiated and observed at 10 K for the external magnetic field H_o // $\langle a \rangle$. The outer portion of the spectrum consists of a doublet of triplets (of spectral extent 13.5 mT) from radical **R1** (the N1 deprotonated uracil cation). The inner portion of the EPR spectrum is a doublet (of spectral extent 1.5 mT) from radical **R6** (the N3 protonated cytosine anion). b) K-band ENDOR spectrum of the EPR spectrum (above) with H_o // $\langle c \rangle$. The magnetic field was positioned on the central doublet (at 855.59 mT). Field-swept ENDOR spectra of the ENDOR lines at 38.96 MHz and at 60.38 MHz gave the same 1.7-mT doublet from radical **R6**. The ENDOR lines shown here between 40 and 45 MHz were too weak to follow as the crystal was rotated. No tensors for these small couplings are given in this study.

close to the intense ENDOR line from the distant protons. It is difficult to follow the angular variations of this ENDOR line at many orientations. However, enough ENDOR measurements were obtained to derive a tentative hyperfine coupling tensor (denoted **6b** in Table 1). As seen in Table 1, the experimental directions of the hyperfine coupling tensor correlate well with the expected directions of an N3−H proton coupling. Therefore it is concluded that radical **R6** is the N3−H protonated cytosine anion, similar to the species previously observed in crystals of various cytosine derivatives.[6]

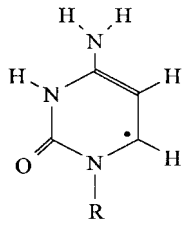

R6

The spin density on C6 can be determined approximately by using the formula $A_{iso} = \rho(C6)Q_{CH}$. Using a Q_{CH} value of −72.8 MHz,[5] ρ(C6) is computed to be 0.53, which is in close agreement with both observed and computed values of other cytosine derivatives.[32] Bernhard has argued that the dipolar coupling tensor is more reliable than the isotropic coupling in calculating π-spin densities in α-carbons.[33] With use of the dipolar coupling tensor, Bernhard's relation yields a spin density of 0.51 at C6.

Attempts were made to determine the fate of radical **R6** by controlled warming experiments. During one experiment **R6** was observed at 10 K and was still present as the crystal was warmed to 77 K. Above this temperature the picture is unclear however because of complications related to overlap from radicals formed upon warming.[2] It should be noted that no H-adducts to the C5=C6 region of cytosine have been observed in this complex at any temperature despite a careful search.

Room-Temperature Results. If a crystal of 1-MeC:5-FU is irradiated at low temperature and warmed to room temperature, the EPR spectrum is dominated by radical **R2**. At the center of the EPR spectrum is a weak doublet (radical **R3**). The general features of these two radicals were discussed previously.[2] A detailed analysis of radical **R3** has now been undertaken. As previously mentioned radical **R3** is best observed in crystals that are freshly irradiated at room temperature.

Typical EPR spectra of radical **R3** were shown previously.[2] For H_o // $\langle b \rangle$ one sees a strong 1.5-mT doublet. For H_o // $\langle a \rangle$ or $\langle c \rangle$ the basic pattern is a 1:2:1 triplet. Generally the EPR pattern consists of two small anisotropic hyperfine couplings. The entire spectrum exhibits a significant *g*-shift, particularly for H_o // $\langle b \rangle$.

No easy analysis of the X-band EPR data was possible because of complications from site splitting and from a mixture of d^+ and d^- transitions.[34] It was therefore necessary to take data at a second microwave frequency (Q-band). At Q-band the EPR spectra due to a relatively small anisotropic hyperfine couplings (ρ(C) < 0.5) are predominately d^- transitions rather than a mixture of d^+ and d^- as is the case at X-band. Using the Q-band spectra a *g*-tensor was derived for radical **R3** (Table 2). The large *g*-anisotropy suggests that this tensor results from a π-radical with significant oxygen spin density.

From the Q-band EPR spectra it was fairly straightforward to see that one hyperfine coupling contributed to the 1:2:1 pattern observed for H_o // $\langle a \rangle$ and $\langle c \rangle$, and collapses to near zero along $\langle b \rangle$. A tensor for this coupling is shown in Table 2 (designated as **3a**).

The second hyperfine coupling was more difficult to determine from the EPR spectra alone because of complications that arose in the crystallographic $\langle bc \rangle$ and $\langle ac \rangle$ planes. Therefore an ENDOR experiment was undertaken. Good ENDOR spectra were observed when H_o // $\langle b \rangle$ for rotation about $\langle a \rangle$ and $\langle c \rangle$. However, in each of these planes when H_o approaches $\langle c \rangle$ or $\langle a \rangle$, respectively, the spectra weakened. No ENDOR spectra were observed in the $\langle ca \rangle$ plane. However, enough data were obtained to derive a hyperfine coupling tensor by using the ENDOR data from the $\langle ab \rangle$ and $\langle bc \rangle$ planes and by using EPR data from the $\langle ca \rangle$ plane. The results are presented in Table 2 (designated as **3b**).

The first entry in Table 2 correlates well with a small F(C5) hyperfine coupling. C5 is in an allylic-type position between C4 and C6, both with large spin densities.[35] The spin density on C5 is therefore small and negative. The fluorine coupling results mainly from spin delocalization through $\pi\pi$-overlap. Thus the fluorine 2pπ spin density is also negative, and the maximum principal value (along the ring normal) therefore is negative.

The eigenvectors corresponding to the minimum and intermediate principal values of the second hyperfine coupling in Table 2 correspond closely with the expected directions of a C6−H coupling.[36] One sees that the eigenvector for the maximum principal value of the *g*-tensor coincides with the direction of the C4=O bond in the native molecule, whereas the eigenvector for the minimum principal value is along the normal to the ring plane. These results therefore suggest that a

TABLE 1: Hyperfine Couplings for Radical R6 formed in 1-MeC:5-FU Single Crystals, X-irradiated, and Observed at 10 K

			eigenvectors[b]			
tensor	isotropic value[a]	principal values	⟨*a*⟩	⟨*b*⟩	⟨*c*⟩	$(\Delta\psi)^c$
		−62.47 ± 0.17	0.5140	−0.4883	−0.7052	
6a	−38.60	−34.58 ± 0.15	0.7847	−0.0643	0.6165	
			(0.7943)	(−0.0315)	(0.6068)[d]	2.0 ± 0.5°
		−18.74 ± 0.12	0.3464	0.8703	−0.3502	
			(0.3003)	(0.8885)	(−0.3470)[e]	2.8 ± 0.3°
		−11.49 ± 0.29	−0.4650	−0.3972	0.7912	
6b	−5.63	−6.41 ± 0.36	0.8636	−0.0071	0.5041	
		1.01 ± 0.32	−0.1946	0.9177	0.3463	
			(−0.3261)	(0.8919)	(0.3134)[f]	8.0 ± 3°

[a] Hyperfine couplings are in MHz. [b] These eigenvectors are for crystallographic site *(l,m,n)*. The other three symmetry-related sites are given by (l, $\bar{m}$, $\bar{n}$), ($\bar{l}$, m, $\bar{n}$), ($\bar{l}$, $\bar{m}$, n). [c] $\Delta\psi$ is the angle between a specific principal value and the expected direction computed from the coordinates of the native molecule.[9] The errors listed for these angles are at the 95% confidence level. [d] The expected direction of the C6 2pπ orbital (the perpendicular to the C5−C6−N1 plane of 1-MeC). [e] The expected direction of the C6−H_α bond (the in-plane bisector of the C5−C6−N1 angle of 1-MeC). [f] The expected direction of the N3−H bond (the in-plane bisector of the C2−N3−C4 bond of 1-MeC).

TABLE 2: Hyperfine Couplings for Radical R3 Formed in 1-MeC:5-FU Single Crystals, X-irradiated, and Observed at Room Temperature

			eigenvectors[b]			
tensor	isotropic value[a]	principal values	⟨*a*⟩	⟨*b*⟩	⟨*c*⟩	$(\Delta\psi)^c$
		−31.64 ± 0.96	0.7861	−0.0283	0.6175	
			(0.8046)	(−0.0060)	(0.5938)[d]	2.1 ± 3.8°
3a	−7.57	8.42 ± 2.8	−0.4513	0.6564	0.6045	
		0.50 ± 4.0	0.4224	0.7539	−0.5032	
		−42.54 ± 0.47	−0.2184	0.9202	0.3249	
3b	−29.37	−32.87 ± 0.24	0.7969	−0.0240	0.6037	
			(0.8183)	(0.0021)	(0.5748)[e]	2.5 ± 0.6°
		−12.71 ± 0.29	−0.5632	−0.3907	0.7280	
			(−0.5339)	(−0.3712)	(0.7597)[f]	2.7 ± 0.6°
		2.0070 ± 0.0001	−0.3288	0.8792	0.3448	
			(−0.2037)	(0.9295)	(0.3076)[g]	8.1 ± 2.2°
g		2.0061 ± 0.0001	−0.5102	−0.4726	0.7186	
		2.0021 ± 0.0001	0.7947	0.0603	0.6039	
			(0.8475)	(−0.0063)	(0.5307)[h]	6.4 ± 0.5°

[a] Hyperfine couplings are in MHz. [b] These eigenvectors are for crystallographic site (l,m,n). The other three symmetry-related sites are given by (l, $\bar{m}$, $\bar{n}$), ($\bar{l}$, m, $\bar{n}$), ($\bar{l}$, $\bar{m}$, n). [c] $\Delta\psi$ is the angle between a specific principal value and the expected direction computed from the coordinates of the native molecule.[9] The errors listed for these angles are at the 95% confidence level. [d] The expected direction of the C5 2pπ orbital (the perpendicular to the C4−C5−C6 plane of 5-FU). [e] The expected direction of the C6 2pπ orbital (the perpendicular to the C5−C6−N1 plane of 5-FU). [f] The expected direction of the C6−H_α bond (the in-plane bisector of the C5−C6−N1 angle of 5-FU). [g] The expected direction of the C4−O4 bond (from the crystal structure). [h] The expected direction of the C4 2pπ orbital (the perpendicular to the N3−C4−C5 plane of 5-FU).

likely free radical model for this room-temperature defect is given as structure **R3**, although no evidence for the additional proton at O4 has been obtained in the present study.

Computed Radical Hyperfine Parameters. The hyperfine coupling constants for the radical cations and anions, as well as all probable neutral radicals formed through net H-atom removal or addition to either of 1-MeC and 5-FU have been calculated. The ionization potentials (IPs) and electron affinities (EAs) of 1-MeC and 5-FU were also computed to determine which base would be oxidized most easily and which base would provide the most favorable electron trap.

The systems investigated are, besides the radical anions and cations of the neutral parent molecules, the H-adducts to positions O2, C5, and C6 of both bases [C•(O2H), C•(C5H), C•(C6H), U•(O2H), U•(C5H), and U•(C6H)], the uracil O4 H-adduct, the uracil N1 and N3 dehydrogenated species, and the C5 defluorinated radical of 5-FU [U•(O4H), U•(−N1H), U•(−N3H), U•(−F5)], and the N3 H-adduct and N4 dehydrogenated radical of 1-MeC [C•(N3H), C•(−N4H)]. The hyperfine couplings and energetics were evaluated both in the presence and absence of a dielectric medium (PCM), and the computed hyperfine couplings were compared with the experimental results described above. To save space, only the systems (and nuclei) relevant for comparisons with the experimental data are listed.

Of the different types of neutral radicals, the most stable forms for 5-FU are the N1 dehydrogenated radical U•(−N1H) and the C5 hydrogenated species U•(C5H). U•(−N3H) is less stable than U•(−N1H) by +25.2 kcal/mol. Compared with U•(C5H), the other hydrogenated species are all less stable [U•(C6H), +0.1 kcal/mol; U•(O4H), +9.7 kcal/mol; U•(O2H), +29.5 kcal/mol]. For 1-MeC, the only dehydrogenated product considered is the N4 form, and of the hydrogenated products, the N3 adduct is the most stable [C•(C5H), +7.9 kcal/mol; C•(C6H), +9.5 kcal/mol; C•(O2H), +13.7 kcal/mol, compared with C•(N3H)].

Table 3 lists the hyperfine couplings for the 5-FU derivatives **R1**, **R2**, and **R3** [U•(−N1H), U•(C6H), and U•(O4H), respectively]. As seen there is a fair agreement between experimental and computed hyperfine couplings for radicals **R1** and **R2**, although the computed fluorine couplings deviate somewhat from the experimental couplings. This is expected because the fluorine couplings are large (47910 MHz for unit 2s spin density on fluorine versus 1420 MHz for unit spin 1s density on a proton, or 1515 MHz for unit 2p coupling in fluorine versus 47.8 MHz for the same coupling with nitrogen). Therefore, small changes in nearby spin densities result in large changes in

TABLE 3: Computed and Experimental Hyperfine Coupling Constants (MHz) for Selected Nuclei of Radicals in 5-FU[a]

radical	nucleus	calc. A_{iso}	calc. dipolar tensor	exp. A_{iso}	exp. dipolar tensor	ref
R1			385.1		322.6	
U(−N1H)	^{19}F5	84.6	−203.3	115.7	−161.7	1
			−181.8		−160.9	
			31.7		26.9	
	^{14}N1	10.9	−16.0	13.5	−13.45	
			−15.7		−13.45	
R2			394.6		327.2	
U(C6H)	^{19}F5	95.8	−212.7	130.6	−196.0	2
			−181.9		−131.2	
	^{1}Hβ1	88.3	(−2.8··+8.4)	89.7		
	^{1}Hβ2	97.8	(−2.8··+8.4)	120.5		
R3			−48.4		−24.1	
(UO4H)	^{19}F5	−20.2	15.1	−7.6	16.0	this work
			33.3		8.1	
			−24.9		−13.2	
	^{1}H6	−41.5	1.4	−29.4	−3.5	
			23.5		16.7	
			−5.3			
	^{1}HO4	−4.76	−4.8			
			10.1			

[a] Calculations were performed using the PCM/B3LYP/6-311G(2df,p) level of theory.

TABLE 4: Computed and Experimental Hyperfine Coupling Constants (MHz) for Selected Nuclei of Radicals in 1-MeC[a]

radical	nucleus	calc. A_{iso}	calc. dipolar tensor	exp. A_{iso}	exp. dipolar tensor	ref
R4			−29.4		−30.0	
C(C6H)	^{1}H5	−45.1	−0.8	−49.9	3.0	4
			30.3		27.0	
	^{1}Hβ1	118.0	(−2.8··+8.4)	133.7		
	^{1}Hβ2	122.5	(−2.8··+8.4)	143.7		
R5			−31.4		−32.2	
C(C5H)	^{1}H6	−43.2	0.6	−48.8	2.6	4
			30.8		29.6	
	^{1}Hβ1	36.7	(−2.8··+8.4)	86.2		
	^{1}Hβ2	127.2	(−2.8··+8.4)	126.5		
R6			−24.6		−23.8	
C(N3H)	^{1}H6	−40.6	2.1	−38.4	3.9	this work
			22.5		19.9	
			4.0			
	^{1}H5	7.0	0.5			
			−4.5			
			9.8		6.6	
	^{1}H(N3)	−8.1	−2.5	−5.6	−0.8	
			−7.3		−5.8	

[a] Calculations were performed using the PCM/B3LYP/6-311G(2df,p) level of theory.

computed fluorine hyperfine couplings. For radical **R3** the computed hyperfine couplings apparently deviate considerably from the experimental values.[36] However, of the full set of systems investigated, no other radical species could be identified showing a better agreement with the observed couplings. In the possible radicals derived from 1-MeC, a far better agreement exists between theory and experiment, as seen from Table 4.

Models for Radical Formation. To determine where the initial, charged, radical centers will be located, the vertical ionization potentials and the vertical and adiabatic electron affinities for the isolated molecules were computed at the B3LYP/6-311+G(2df,p) level, using the B3LYP/6-31G(d,p) optimized geometries. The data obtained imply that the initial cationic centers will be formed on 1-MeC (IP = 195.9 kcal/mol, compared with 218.1 kcal/mol for 5-FU). The ejected electrons, on the other hand, will be captured primarily by the uracils, because both the vertical and adiabatic EAs are 11 kcal/mol more stable for 5-FU than for 1-MeC. The vertical electron affinity for 5-FU is only +1.43 kcal/mol, and becomes −7.7 kcal/mol after geometric relaxation (i.e., more stable than the neutral parent). These findings are in agreement with recent detailed computations illustrating the importance of diffuse functions for accurate EAs of the nucleotides.[37]

These theoretical results appear to be at odds with the experimental results. The detection of radical **R1** suggests a parent uracil cation, whereas radical **R6** suggests a parent cytosine anion. The actual parent ions were not observed experimentally at 10 K. One observes only radicals stabilized after protonation/deprotonation reactions. Therefore it is important to perform the above-mentioned calculations on entire base pairs to analyze the stabilities of the possible charged centers after protonation/deprotonation rearrangements in the cocrystalline system. Various combinations of base pairs in Figure 2 were considered for these calculations.

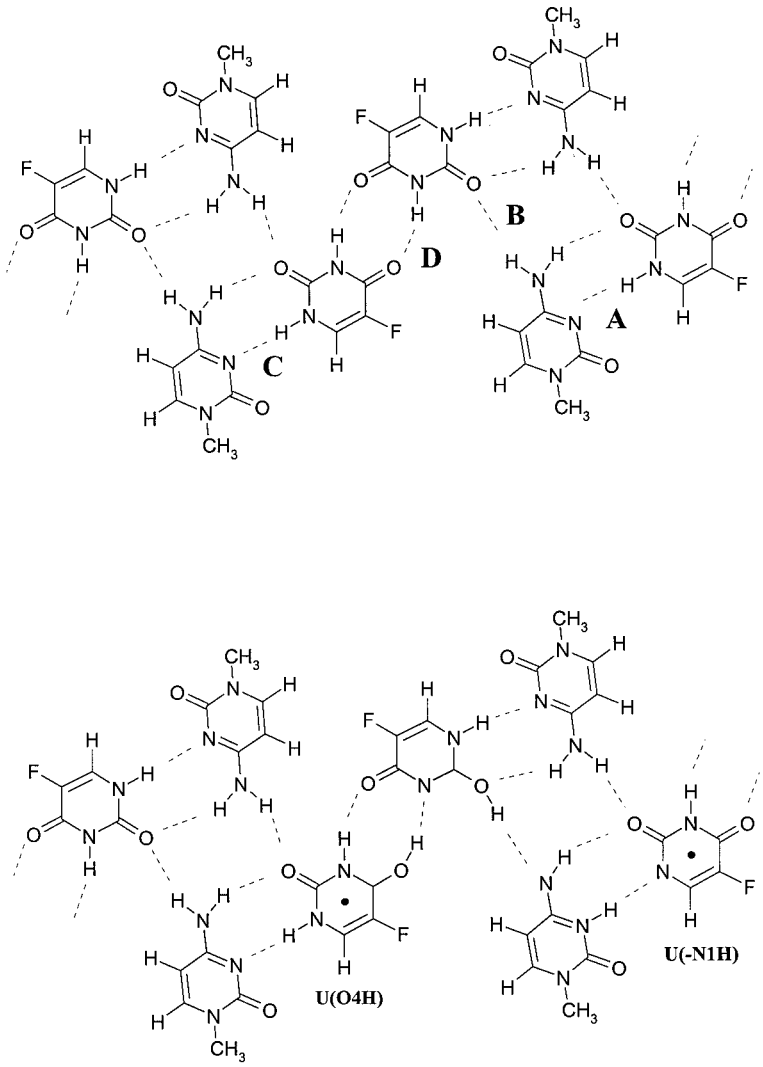

Figure 2. Model of the 1-MeC:5-FU crystal (see ref 9). (top) Areas indicating (A) C−U cation dimer, (B) site of deprotonation of the cytosine cation, (C) C−U anion dimer, and (D) site of protonation of the uracil anion. Charge neutralization occurs at the upper uracil molecule. (bottom) Hydrogen bonding and protonation pattern after deprotonation of the uracil cation U•(−N1H) radical **R1**, and formation of the U•(O4H) radical **R3**.

The calculations on the full C−U cation radical dimer (segment A in Figure 2), indicate that upon oxidation of this dimer, uracil will deprotonate spontaneously and without barrier at the N1 position (to N3 of the cytosine) to produce radical **R1** and the cationic $C(N3H)^+$ species. That is, starting from a neutral optimized dimer structure, the ionized dimer will optimize to the U•(−N1H) + $C(N3H)^+$ proton-transfer pair in just a few iterations without passing over any significant energy barrier. This trend is verified by considering the energetics of the isolated reactants [C + $U^{\bullet+}$ vs $C(N3H)^+$ + U•(−N1H)], which is exothermic by 35.2 kcal/mol. The energetics of this reaction sequence are displayed in Figure 3 where the overall mechanism is also broken down into subprocesses by considering the isolated reactants. It is suggested that a charge transfer to U is taking place $C^{\bullet+}$ +U vs C + $U^{\bullet+}$ which, considering the isolated reactants, is endothermic by 18.3 kcal/mol) followed by a proton transfer from $U^{\bullet+}$ to C. Alternatively, the entire process may be regarded as H-atom (radical) transfer. The cationic $C(N3H)^+$ may now deprotonate at N4, to the O2 position of an adjacent U (step B of Figure 2). This step is endothermic by 42 kcal/mol. Thus the two-step process [deprotonation of $U^{\bullet+}$, followed by deprotonation of $C(N3H)^+$] is endothermic by ca.. 7 kcal/mol. Alternatively, $C(N3H)^+$ may undergo proton transfer to charge neutralize an adjacent U(−N3H)$^-$ anion, as outlined below.

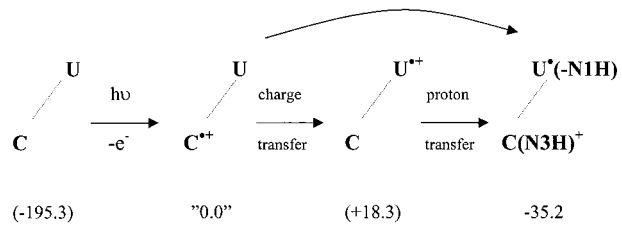

Figure 3. Schematic overview of the different steps leading to formation of the U•(−N1H) radical (**R1**) from the cationic radical center. $C(N3H)^+$ may subsequently undergo charge neutralization with the uracil tautomer anion formed from the anionic radical center. Relative energies (in kcal/mol) are computed from calculations on isolated molecules.

The fate of the primary reduction product has been determined by calculations of a negatively charged C−U dimer (C of Figure 2). This dimer was also found to undergo a barrier-free deprotonation of uracil, to form the neutral C•(N3H) adduct radical **R6** and the anionic U(−N1H)$^-$ moiety. Again, the overall mechanism may be broken down into subprocesses by considering the isolated reactants (Figure 4). Localizing the unpaired electron on U is ca. 10 kcal/mol more stable than on C (i.e., C + $U^{\bullet-}$ vs $C^{\bullet-}$ + U is endothermic by 10 kcal/mol).

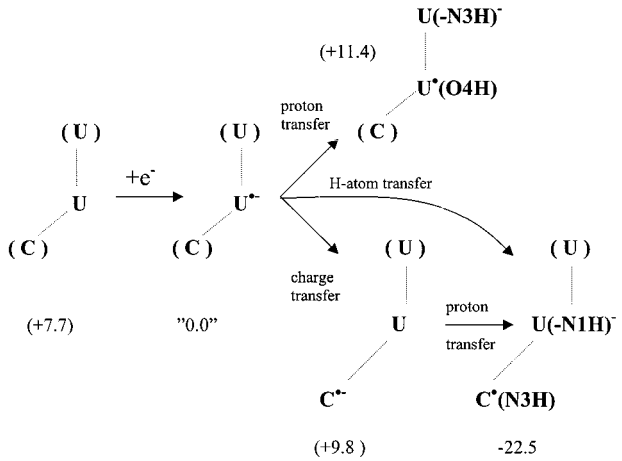

Figure 4. Possible transfer mechanism from the anionic radical center in the 1-MeC:5-FU cocrystal leading to formation of the U•(O4H) radical (**R3**) or, via subsequent H-atom transfer from C•(N3H), the U•(C6H) radical (**R2**). Relative energies (in kcal/mol) are computed from calculations on isolated molecules.

The uracil anion radical now has two choices. It may either transfer its excess electron to cytosine (endothermic by 10 kcal/mol), followed by a 32 kcal/mol exothermic proton-transfer step to form C•(N3H) (**R6**) and U(−N1H)⁻, as observed when considering the full dimer C−U anion radical. Again the process alternatively may be viewed as a radical (H-atom) transfer. The U(−N1H)⁻ anion may now accept a proton from the adjacent uracil to form the neutral U(−N1H,+O4H) tautomer (step D of Figure 2), whereafter the newly formed uracil anion U(−N3H)⁻ can undergo charge neutralization with the cationic C(N3H)⁺ formed from the above-described cationic charge center. However, other options may exist. The initial uracil anion radical may protonate from the adjacent uracil to form the observed neutral U•(O4H) adduct radical (**R3**) and the U(−N3H)⁻ anion. This process is endothermic by 11.4 kcal/mol, that is, essentially the same amount as for the U → C charge transfer (see Figure 4). Thus having formed the U(−N3H)⁻ anion and the above-mentioned C(N3H)⁺, these will also undergo an exothermic charge neutralization (proton transfer) to form the two neutral tautomers U(−N3H, +O2H) and C(+N3H, −N4), with ΔE −93.5 kcal/mol.

The final radical transfer step involves formation of the U•(C6H) adduct (**R2**) from C•(N3H). As seen in Figure 4, C•(N3H) can be formed in the electron + proton-transfer process of the C−U dimer. In cytosine, the $-N4H_2$ amino group is slightly nonplanar. Assuming the C•(N3H) radical is formed with excess energy, this may be sufficient to eject one of the (out-of-plane) amino H-atoms to add to the C6 position of a uracil of the next layer in the crystal (because the C:U layers are arranged in a graphite-like sheet structure). Energetically, the process C•(N3H) + U → C(+N3H,−N4H) + U•(C6H) is endothermic by only 3 kcal/mol, and since the formation of C•(N3H) from C•⁻ + U in itself is exothermic by 22.5 kcal/mol, there should be sufficient surplus energy available in the system.

Discussion

This and the two previous studies of 1-MeC:5-FU present a fairly complete picture of the radicals trapped in this irradiated cocrystal. At the lowest temperatures available (10 K) one sees mainly products that result from oxidation of uracil (**R1**) and reduction of cytosine (**R6**). At 77 K one sees radical **R2**, formed by net H-addition to 5-FU. So now one can ask why only these radicals are stabilized in this cocrystal.

Bernhard has studied the influence of hydrogen-bonding networks, which promote the trapping of radicals through reversible proton transfer, on radical yields.[38] Figure 2 shows how the 1-MeC:5-FU base pair is hydrogen bonded to various neighbors. In the previous section theoretical calculations were presented which consider the consequences of 5-FU oxidation and 1-MeC reduction. The calculations showed that it is energetically favorable for the hydrogen-bonding matrix to stably trap radicals **R1** and **R6**.

The purpose of the theoretical calculations discussed above was to show what may be the fates of the primary oxidation and reduction products in 1-MeC:5-FU. The calculations seem to support the experimental observations that only radicals **R1** and **R6** are stabilized at 10 K. One could ask about alternative schemes. Is there a similar proton shuttle scheme that would stabilize an oxidation product on cytosine and a reduction product on uracil? Calculations show that C•⁺+ U → C•(−N4H) + U(O2H)⁺ is endothermic by 37.4 kcal/mol. Likewise, calculations show that U•⁻ + C → U•(O2H) + C(−N4H)⁻ is endothermic by 38.7 kcal/mol. This means that it is not energetically favorable for either the cytosine cation to deprotonate or the uracil anion to protonate in the hydrogen-bonding arrangement found in 1-MeC:5-FU.

One can further put this proposed scheme into perspective by looking at the dose-response curves of the cocrystal. The average free radical yield at 4 K for 1-MeC:5-FU is 0.038 ± 0.009 μmol/J.[13] This value is 1 order of magnitude less than in DNA, about one third that of cytosine monohydrate, but about 100 times that of 1-MeC alone.[8] This therefore is a relatively high free radical yield, and makes the electron transfer/proton shuttle schemes discussed above seem like reasonable possibilities.

Next the fates of radicals **R1** and **R6** upon warming are considered. While the fate of radical **R6** is unclear, it is clear that no cytosine C5 or C6 H-addition radicals are observed upon warming from 10 K. Also no cytosine H-adducts were formed by irradiation at 77 K or by irradiation at room temperature. If they are formed, they are easy to detect by EPR because their spectral features have been well characterized.[4] Because these H-addition radicals are not observed, one must ask why the behavior of 1-MeC is different in the cocrystal of 1-MeC:5-FU.

Previous work on a wide variety of alkenes has shown that the barrier to H-addition over a double bond is very small (in the range of 1−2 kcal/mol[39]). The same holds for H-addition to the C5 and C6 positions in thymine.[40] The product distribution must in this case primarily be thermodynamically driven, because we may expect differences in barriers heights to be very small. Comparing the relative stabilities of the H-adducts at C5 and C6 for both 5-FU and 1-MeC, one notes that the product energies of the two addition sites within each system are essentially degenerate. However, the uracil adducts are 8−10 kcal/mol more stable relative to the parent molecule, than are the corresponding cytosine adducts. This may explain the observation that only uracil H-adducts (to the C5=C6 double bond) are seen in the 1-MeC:5-FU cocrystals.[41]

Radical **R3** has features in common with a model proposed for a similar radical observed in 5-FU by Neumüller and Hüttermann.[7] In that analysis an additional C4−OH coupling was reported, which collapsed upon deuteration. In the present analysis, no additional C4−OH coupling was observed for radical **R3**. Indeed the EPR spectra in crystals prepared from H_2O and D_2O appeared to be identical. This means that either

the deuteration at this site was ineffective, or more likely that the proton lies in the nodal plane.

In the previous study of 5-FU the authors argue that the OH proton is in the ring plane (dihedral angle $\theta = 90°$), although a significant $a_{iso} = -10.1$ MHz for this proton coupling is reported. (The hyperfine tensor for the C4−OH coupling is given in this reference as −4.76, −14.0, and −11.5 MHz. The dipolar couplings are 5.3, −3.9, and −1.4 MHz.[7]) The theoretical calculation for this coupling (with the C4−OH proton in the molecular plane) yields −4.76 MHz as shown in Table 3. An independent model calculation of the dipolar coupling tensor[42] for the C4−OH coupling, assuming $\rho^{\pi}(C4) = 0.45$, $\rho^{\pi}(O4) = -0.02$, and a dihedral angle $\theta = 90°$, yields a dipolar tensor with diagonal elements 7.90, −2.77, and −5.14 MHz, in essential agreement with the DFT calculations. These results suggest that if the C4−OH proton is indeed in the ring plane, then the isotropic hyperfine coupling should be small.

From the above it is seen that it is possible to explain, from energetic arguments, the formation of the 5-FU derived radicals (**R1**, **R2**, and **R3**) in the 1-MeC:5-FU cocrystals. Although there is initial radiation damage to the cytosine moiety (**R6**), there is no evidence of any cytosine H-addition radicals that one usually sees in irradiated cytosine derivatives. This therefore is a clear case in which the radiation chemistry of one base is modified in the presence of another base.

Acknowledgment. This work is supported by PHS Grant R01 CA36810-14 awarded by the National Cancer Institute, DHHS. The contents of this paper are solely the responsibility of the authors and do not necessarily represent the official view of the National Cancer Institute. Partial support came from NATO Travel Grant 0426/88. L.A.E. gratefully acknowledges the Swedish Natural Sciences Research Council (NFR) for financial support, and the Center for Parallel Computing (PDC) in Stockholm for grants of computer time. We thank William Bernhard and Michael Debije at the University of Rochester for measuring the free radical yields in 1-MeC:5-FU, and also for many helpful discussions.

References and Notes

(1) Farley, R. A.; Bernhard, W. A. *Radiat. Res.* **1975**, *61*, 47.
(2) Close, D. M.; Farley, R. A.; Bernhard, W. A. *Radiat. Res.* **1978**, *73*, 212.
(3) Wyard, S. J.; Elliott, J. P. *Ann. N.Y. Acad. Sci.* **1968**, *222*, 628.
(4) Rustgi, S. N.; Box, H. C. *J. Chem. Phys.* **1974**, *60*, 3343. In this short paper the irradiation temperature is not given. Upon request Prof. Box has informed us that the 1-MeC crystals were irradiated at room temperature and examined with the V-band EPR spectrometer at 4.2 K.
(5) Bernhard, W. A. *Adv. Radiat. Biol.* **1981**, *9*, 199.
(6) Close, D. M.; Hole, E. O.; Sagstuen, E.; Nelson, W. H. *J. Phys. Chem.* **1998**, *102*, 6737.
(7) Neumüller, W.; Hüttermann, J. *Int. J. Radiat. Biol.* **1980**, *37*, 49.
(8) Bernhard, W. A.; Barnes, J.; Mercer, K. M.; Mroczka, N. *Radiat. Res.* **1994**, *140*, 199.
(9) Kim, S. H.; Rich, A. *J. Mol. Biol.* **1969**, *42*, 87.
(10) Busing, W. R.; Martin, K. O.; Levy, H. A. *Oak Ridge National Laboratories. ONRL-TM-306* 1964.
(11) Close, D. M.; Fouse, G. W.; Bernhard, W. A. *J. Chem. Phys.* **1977**, *66*, 1534.
(12) Nelson, W. H.; Hole, E. O.; Sagstuen, E.; Close, D. M. *Int. J. Radiat. Biol.* **1988**, *54*, 963.
(13) The free radical yield in the 1-MeC:5-FU crystals was measured by William Bernhard and Michael Debije at the University of Rochester.
(14) Becke, A. D. *J. Chem. Phys.* **1993**, *98*, 5648.
(15) Devlin, P. J.; Chabloski, C. F.; Frisch, M. J. *J. Phys. Chem.* **1994**, *98*, 11623.
(16) Lee, C.; Yang, W.; Parr, R. G. *Phys. Rev.* **1988**, *B37*, 785.
(17) Krishnan, R.; Binkley, J. S.; Pople, J. A. *J. Chem. Phys.* **1980**, *72*, 650.
(18) McLean, A. D.; Chandler, G. S. *J. Chem. Phys.* **1980**, *72*, 5639.
(19) Frisch, M. J.; Binkley, J. S.; Pople, J. A. *J. Chem. Phys.* **1984**, *80*, 3265.
(20) Barone, V.; Cossi, M.; Tomasi, J. *J. Comput. Chem.* **1998**, *19*, 404.
(21) Cances, M. T.; Mennucci, V.; Tomasi, J. *J. Chem. Phys.* **1997**, *107*, 3032.
(22) Cossi, M.; Barone, V.; Cammi, R.; Tomasi, J. *Chem. Phys. Lett.* **1996**, *255*, 327.
(23) Miertus, S.; Scrocco, E.; Tomasi, J. *J. Chem. Phys.* **1981**, *55*, 117.
(24) Foresman, J. B.; Keith, T. A.; Wiberg, K. B.; Snoonian, J.; Frisch, M. J. *J. Phys. Chem.* **1996**, *100*, 16098.
(25) Frisch, M. J.; Trucks, G. W.; Schlegel, H. B.; Scuseria, G. E.; Robb, M. A.; Cheeseman, J. R.; Zakrzewski, V. G.; Montgomery, J. A., Jr.; Stratmann, R. E.; Burant, J. C.; Dapprich, S.; Millam, J. M.; Daniels, A. D.; Kudin, K. N.; Strain, M. C.; Farkas, O.; Tomasi, J.; Barone, V.; Cossi, M.; Cammi, R.; Mennucci, B.; Pomelli, C.; Adamo, C.; Clifford, S.; Ochterski, J.; Petersson, G. A.; Ayala, P. Y.; Cui, Q.; Morokuma, K.; Malick, D. K.; Rabuck, A. D.; Raghavachari, K.; Foresman, J. B.; Cioslowski, J.; Ortiz, J. V.; Stefanov, B. B.; Liu, G.; Liashenko, A.; Piskorz, P.; Komaromi, I.; Gomperts, R.; Martin, R. L.; Fox, D. J.; Keith, T.; Al-Laham, M. A.; Peng, C. Y.; Nanayakkara, A.; Gonzalez, C.; Challacombe, M.; Gill, P. M. W.; Johnson, G.; Chen, W.; Wong, M. W.; Andres, J. L.; Gonzalez, C.; Head-Gordon, M.; Replogle, E. A.; Pople, J. A. *Gaussian 98* (Revision A.6); Gaussian, Inc.: Pittsburgh, PA, 1998.
(26) Wetmore, S. D.; Himo, F.; Boyd, R. J.; Eriksson, L. A. *J. Phys. Chem. B* **1998**, *102*, 7484.
(27) Wetmore, S. D.; Boyd, R. J.; Eriksson, L. A. *J. Phys. Chem. B* **1998**, *102*, 5369.
(28) Lassmann, G.; Eriksson, L. A.; Himo, F.; Lendzian, F.; Lubitz, W. *J. Phys. Chem. A* **1999**, *103*, 1283.
(29) Llano, J.; Eriksson, L. A. *J. Phys. Chem. B* **1999**, *103*, 5598.
(30) Malkin, V., G.; Malkina, O. L.; Eriksson, L. A.; Salahub, D. R. *Theoretical and Computational Chemistry*: *Vol. 2, Modern Density Functional Theory-A Tool for Chemistry*; Politzer, P., Seminario, J. M., Eds.; Elsevier: Amsterdam, 1995; pp 273−346.
(31) Barone, V. In *Recent Advances in Density Functional Theory*; Chong, D. P., Ed.; World Scientific: Singapore, 1995, Part 1, pp 287−334.
(32) Close, D. M. *Radiat. Res.* **1993**, *135*, 1.
(33) Bernhard, W. A. *J. Chem. Phys.* **1984**, *81*, 5928.
(34) Miyagawa, I.; Gordy, W. *J. Chem. Phys.* **1960**, *32*, 255. The notation here is to designate the outer pair of the four allowed EPR transitions as d^+, and the inner pair as d^-.
(35) Heller, C.; Cole, T. *J. Chem. Phys.* **1962**, *37*, 243.
(36) Comparing the tensor here with the hyperfine couplings from a normal C6−H_α coupling, one might expect the largest principal value to be more like 50 MHz. The somewhat smaller experimental value presented here most likely results from difficulties in following the experimental data.
(37) Wetmore, S. D.; Boyd, R. J.; Eriksson, L. A. *Chem. Phys. Lett.* **2000**, *322*, 129.
(38) Bernhard, W. A.; Mroczka, N.; Barnes, J. *Int. J. Radiat. Biol.* **1994**, *66*, 491.
(39) Werst, D. W.; Han, P.; Choure, S. C.; Vinokur, E. I.; Xu, L.; Trifunac, A. D.; Eriksson, L. A. *J. Phys. Chem. B* **1999**, *103*, 9219.
(40) Grand, A. Private communication.
(41) It should be emphasized, that, in the energetics above, the fact that in the crystal structures the uracils form five hydrogen bonds, whereas the cytosines form only three (cf. Figure 2) has not been considered explicitly, but only via the polarized continuum model.
(42) Sagstuen, E.; Awadelkarim, O.; Lund, A.; Masiakowski, J. *J. Chem. Phys.* **1986**, *85*, 3223.